CFD studies on natural convection heat transfer of Al$_2$O$_3$-water nanofluids

W. Rashmi, A. F. Ismail, M. Khalid & Y. Faridah

Springer

ORIGINAL

CFD studies on natural convection heat transfer of Al₂O₃-water nanofluids

W. Rashmi · A. F. Ismail · M. Khalid · Y. Faridah

Abstract This work is focused on numerical simulations of natural convection heat transfer in Al₂O₃-water nanofluids using computational fluid dynamics approach. Fluent v6.3 is used to simulate water based nanofluid considering it as a single phase. Thermo-physical properties of the nanofluids are considered in terms of volume fraction and size of nanoparticles, size of base fluid molecule and temperature. The numerical values of effective thermal conductivity have also been compared with the experimental values available in the literature. The numerical result simulated shows decrease in heat transfer with increase in particle volume fraction. Computed result shows similar trend in increase of Nusselt number with Relayigh number as depicted by experimental results. Streamlines and temperature profiles are plotted to demonstrate the effect.

List of symbols

A_m Surface area of the fluid particle
C_{pf} Specific heat of fluid
C_{pp} Specific heat of particle
g Acceleration due to gravity
h Heat transfer coefficient
T_H Temperature of hot wall
T_L Temperature of cold wall
k_{eff} Effective thermal conductivity
k_f Thermal conductivity of the fluid
k_p Thermal conductivity of nanoparticle
L Length of the cylindrical fluid container

N_u Nusselt number
Q Input power
r_p Radius of fluid particle
R_a Rayleigh number
T Nanofluid temperature
T_{ref} Reference temperature (293 K)
μ_f Viscosity of the base fluid
μ_o Reference viscosity of water
ρ_f Density of fluid
ρ Density
ρ_p Density of nanoparticle
φ Volume fraction of nanoparticle
η_n Kinematic viscosity of the nanofluid
α_n Thermal diffusivity of the nanofluid

W. Rashmi (✉) · A. F. Ismail · M. Khalid · Y. Faridah
Nanoscience and Nanotechnology Research Group (NANORG),
International Islamic University Malaysia, P. O Box 10,
50728 Kuala Lumpur, Malaysia
e-mail: rashmi.walvekar@gmail.com

1 Introduction

Conventional fluids, such as water, engine oil and ethylene glycol are normally used as heat transfer fluids. Although various techniques are applied to enhance the heat transfer, the lower heat transfer performance of these conventional fluids obstructs the performance enhancement and the compactness of heat exchangers. The use of solid particles as an additive suspended into the base fluid is a technique for the heat transfer enhancement. Nanofluids are dispersions of nanometer sized particles (metallic or non-metallic) in base fluid such as water, ethylene glycol, synthetic oil etc. The enhancement of thermal conductivity of conventional fluids by the suspension of solid particles, such as millimeter- or micrometer-sized particles, has been well known for more than a century [1]. Considering that the nanofluid heat capacity is not enhanced but diminished, the

presence of nanoparticles significantly enhances the transport and thermal properties of the base fluid. For example, Xuan and Li [2] experimentally studied on the thermal conductivity of a nanofluid consisting of copper nanoparticles and base liquid. Their data showed that the suspended nanoparticles obviously increased the thermal conductivity of the base liquid. Thermal conductivity of the nanofluid increased with increasing volume fraction of nanoparticles. For instance, the ratio of thermal conductivity of Cu–water to that of the base liquid increased from 1.24 to 1.78 when the volume fraction of the nanoparticles varied from 2.5 to 7.5%. Similar behaviour were reported by Eastman et al. [3], who obtained 60% increase in thermal conductivity with 5 vol% of CuO nanoparticles dispersed in water. Further, it was reported that a small amount (<1% volume fraction) of copper or carbon nanotube nanoparticles suspended in ethylene glycol or oil increased thermal conductivity by 40 and 150% [4, 5]. Similarly, two to fourfold increase in thermal conductivity was observed by Das et al. [6] over a temperature range of 21–51°C for water based nanofluids for Al_2O_3 or CuO nanoparticles.

It is evident from the literature that the thermal conductivity of nanofluids is a function of thermal conductivity (of both the base fluid and the nanoparticle material), the volume fraction, the surface area, and the shape of the nanoparticles suspended in the base liquid. There are no theoretical formulas currently available in open literature for the accurate prediction of the thermal conductivity of nanofluids. Several studies on convective heat transfer of nanofluids have been reported in literature. For instance, buoyancy driven heat transfer in nanofluids in 2-dimensional enclosure was reported by Khanafer et al. [7]. Jang and Choi [8] studied free convection in a rectangular cavity. Similarly, Jou and Tzeng [9] reported numerical results on heat transfer enhancement of nanofluids in 2-dimensional enclosure. They reported an increase in heat transfer rate with increase in particle volume fraction. Santra et al. [10] studied heat transfer rate in a differentially heated square cavity using Cu-water nanofluid. Hwang et al. [11] theoretically investigated natural convection of alumina-water nanofluid in a rectangular cavity. With regards to the CFD simulations using FLUENT software, Jafari et al. [12] studied the effect of gravity on sedimentation and clustering of nano ferro-fluids on natural convection heat transfer. They used both the single phase approach and mixture model. Buoyancy driven heat transfer of nanofluids was studied by Ismail et al. [13] using FLUENT. Effect of volume fraction and Rayleigh number was studies in their work using single phase approach.

Review of the pertinent literature on the heat transfer characteristics of nanofluids shows that, over the years, considerable efforts have been given to investigate this problem experimentally, however, very few studies relates to numerical investigations on natural convection heat transfer. Therefore, the objective of this work is to numerically simulate natural convective heat transfer of nanofluids and validate them with the previous experimental results. The numerical simulations were carried out using the computational fluid dynamic (CFD) approach. CFD is a technique or a tool which enables us to study the fluid flow, heat transfer and associated phenomena based on computer simulations. In this study, commercial CFD software (FLUENT v6.3) is employed to study natural convection heat transfer of nanofluids. Simulations have been carried out in a geometry of L/D = 1.0, as used in the experimental setup of Putra et al. [14]. The geometry is an enclosed cylinder containing nanofluid enclosed by hot and cold walls on right and left, respectively, and curved wall is adiabatic surface. The numerical results are presented in terms of non-dimensional parameters such as Nusselt number and Rayleigh number. Theoretical models for thermal conductivity, viscosity of base fluid, effective viscosity, specific heat, density using Boussinesq approximation are employed using user defined function (UDF) in the FLUENT v6.3.

2 Thermo-physical properties of Al_2O_3-water nanofluids

The fluid properties of the nanofluids vary when nanoparticles are suspended in them. There are two ways to describe material properties of the nanofluid. First is to assume the nanofluid as a mixture of two fluids and secondly to treat them as single phase. Former is used due to its accuracy. In this work, two theoretical models: Kinetic model and interfacial model are used to calculate the thermal conductivity of the nanofluid.

2.1 Thermal conductivity

Two different models are used in present work to approximate effective thermal conductivity of nanofluids. Maxwell–Garnett model [15] and Kinetic model [16] as given by Eqs. 1 and 2, respectively.

2.1.1 Maxwell–Garnett model of thermal conductivity

$$k_{\text{eff}} = \frac{k_p + 2k_f - 2\phi(k_f - k_p)}{k_p + 2k_f + \phi(k_f - k_p)} \tag{1}$$

2.1.2 Kinetic model

There are two types of kinetic model proposed in the literature [16]. One assumes that the particles are stationary (stationary particle model) and other assumes that the

particles are in motion (moving particle model) inside the base fluid. In this study, stationary particle model is employed in the numerical simulations.

$$k_{\text{eff}} = k_f \left[1 + \frac{k_p \phi \, r_f}{k_f (1 - \phi) r_p} \right] \qquad (2)$$

Equation 2 is used in numerical simulations to compute the thermal conductivity of the nanofluid. The radius of the fluid (water) particle used is 3.2×10^{-10} m and that of Al_2O_3 nanoparticle is 131.2×10^{-9} m was used [14].

2.2 Density

The density of the nanofluid is expressed in terms of density of fluid, density of nanoparticles, and volume fraction of nanoparticles as given in Eq. 3;

$$\rho = (1 - \phi) \rho_f + \phi \rho_p \qquad (3)$$

Equation 3 shows that the density of nanofluid increases with increase in volume fraction of nanoparticles.

2.3 Specific heat

The specific heat of nanofluid is given by,

$$C_p = \frac{(1 - \phi) \rho_f C_{pf} + \phi \rho_p C_{pp}}{\rho} \qquad (4)$$

Equation 4 predicts small decrease in specific heat of the nanofluid with increase in nanoparticle volume fraction.

2.4 Viscosity

The viscosity of the nanofluid increases with increase in the nanoparticle concentration. For low volume fraction of nanoparticles, Einstein's model can be used to predict the viscosity of the nanofluid as given in Eqs. 5 and 6.

$$\mu_n = (1 + 2.5\phi) \mu_f \qquad (5)$$

where,

$$\mu_f = \mu_o \left[e^{-1.704 - 5.306 \left(\frac{T_{\text{ref}}}{T} \right) + 7.003 \left(\frac{T_{\text{ref}}}{T} \right)^2} \right] \qquad (6)$$

Equation 5 shows the dependence of viscosity of base fluid on temperature. Einsteins's equation is valid only for small volume fraction of nanoparticles ($\phi < 0.05$). It is applicable for the numerical simulations performed in this work as the maximum volume fraction of nanoparticles is 0.04.

2.5 Thermal expansion coefficient

The thermal expansion coefficient is considered to be independent of volume fraction of the nanoparticles. It is dependent only on temperature of the base fluid. In this

Table 1 Values of thermal expansion coefficient used in numerical simulations [15]

Average temperature (K)	Thermal expansion coefficient, β (1/K)
298.15	0.0002
307.55	0.0003
315.55	0.0004

work, the values of thermal expansion coefficient are calculated based on the average temperature between hot and cold walls. The values of thermal expansion coefficient used in this study are tabulated in Table 1. Thermo-physical properties of the nanofluid at different particle concentration and average temperature of the base fluid used in the present work are tabulated in Table 2.

3 CFD simulation

3.1 Geometry creation and grid arrangement

The geometry and the grid were generated using preprocessor called GAMBIT. It is an integrated preprocessor for CFD analysis. The geometry and the grid are shown in Figs. 1 and 2, respectively.

The physical boundary conditions for the geometry are defined as hot wall (left), cold wall (right) and adiabatic wall (top and bottom). The continuum was defined as fluid. The mesh file was further exported to FLUENT.

4 Computational model

4.1 Assumptions

The nanoparticles in the base fluid can be easily fluidized and, thus, the nanofluid mixture is considered as a single phase. It is also assumed that the nanoparticles and the base fluid are in thermal equilibrium with each other and thus the relative velocity is negligible or equal to zero. The effective thermo-physical properties depend upon the temperature and volume concentration of the nanoparticles and properties of both base fluid and suspended particles. Thus, the well known equation of single phase flow (i.e., equations of conservation of mass, momentum and energy) can be readily extended and employed for nanofluids.

4.2 Numerical method

In this study, both the phases are considered as a single phase. The model equations can be written as below.

Table 2 Thermo-physical properties of Al$_2$O$_3$-water nanofluids

Fluid	Density (kg/m3)	Specific heat (J/kgK)	Thermal conductivity (W/mK)	Viscosity (Pa s)
Nanofluid properties				
Pure water				
At Tavg = 298.15 K	997.13	4,180	0.613	0.000891
At Tavg = 307.55 K	994.43	4,178	0.613	0.000734
At Tavg = 315.55 K	991.46	4,179	0.613	0.000629
Al$_2$O$_3$	3,970	765	40	–
Water + 1% Al$_2$O$_3$				
At Tavg = 298.15 K	1,026.86	4,047.97	0.615, 0.628	0.0009132
At Tavg = 307.55 K	1,024.18	4,045.7	0.615, 0.628	0.0007523
At Tavg = 315.55 K	1,021.25	4,046.28	0.615, 0.628	0.0006447
Water + 4% Al$_2$O$_3$				
At Tavg = 298.15 K	1,116.04	3,694.08	0.621, 0.683	0.0009801
At Tavg = 307.55 K	1,113.45	3,691.24	0.621, 0.683	0.0008074
At Tavg = 315.55 K	1,110.6	3,690.84	0.621, 0.683	0.0006919
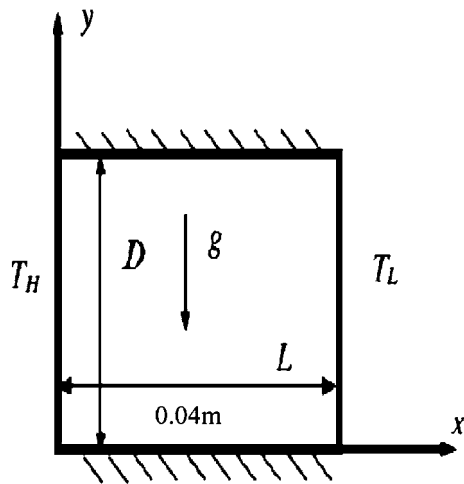
Fig. 1 Schematic representation of two-dimensional enclosure
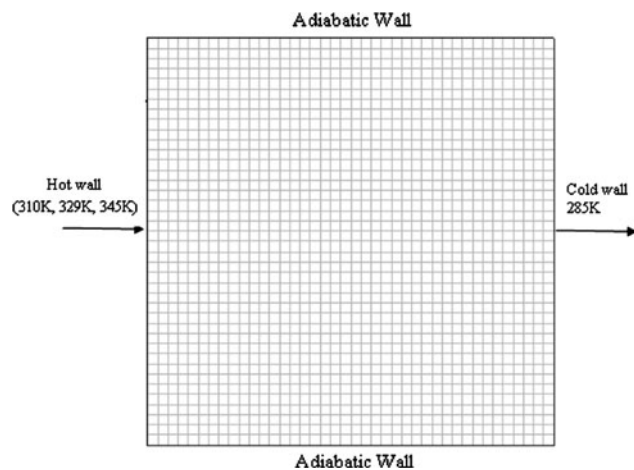
Fig. 2 Uniform grid generated using Gambit

Continuity equation

$$\frac{\partial}{\partial t}(\rho_n) + \nabla \cdot (\rho_n \cdot \bar{v}_n) = 0 \tag{7}$$

Momentum equation

$$\frac{\partial}{\partial t}(\rho_n v_n) + (\rho_n v_n v_n) = -\nabla p + \nabla \cdot \left[\mu_n\left(\nabla v_n + \nabla v_n^T\right)\right] + \rho_n g$$
$$+ F + \nabla \cdot \left(\sum_{k=1}^{n} \phi_k \rho_k v_{dr\,k} v_{drk}\right) \tag{8}$$

Energy equation

$$\frac{\partial}{\partial t}\left(\sum_{k=1}^{n} \phi_k \rho_k h_k\right) + \nabla \cdot \sum_{k=1}^{n}(\phi_k v_k(\rho_k h_k + p))$$
$$= \nabla \cdot (k_{\text{eff}} \nabla T) \tag{9}$$

The governing equations of fluid flow were numerically solved using segregated solver. Time independent (steady state) solver was used for all the simulations. Laminar model was used to simulate the natural convection flow using SIMPLE scheme for pressure–velocity coupling and PRESTO was used for pressure. All the material properties described in Sect. 2 are input using User Defined Function (UDF). Second order discretization scheme were employed for all simulations. Iterations were performed using Gauss–Siedal method until all the residuals reached below 1×10^{-6}. All material properties, initial values of temperatures and volume fraction were provided to run the simulations in FLUENT. The output from the simulations was then used to compare the results with previous experimental results.

The total surface heat flux (Q) was computed from hot wall in each case using surface integrals. Heat transfer coefficient was then calculated using the value of total

surface heat flux as given in Eq. 10. Nusselt number and Rayleigh number were then computed using Eqs. 11 and 12 and the material properties of the nanofluids obtained from UDF's. Plots of Nusselt number vs Rayleigh number were obtained for Al_2O_3-water nanofluid for 0, 1 and 4% volume fraction and for cylinder of aspect ratio of L/D = 1.0

$$h = \frac{4Q}{\pi d^2 (T_H - T_c)} \quad (10)$$

$$Nu = \frac{hL}{k_n} \quad (11)$$

$$Ra = \frac{g\beta_n \Delta T L^3}{\eta_n \alpha_n} \quad (12)$$

5 Results and discussion

5.1 Grid independent study

Prior to performing the actual simulations on nanofluids flow, grid independence study was carried out with three different (41×41, 61×61, and 81×81) grid sizes. These studies are performed for pure water. The hot and cold walls are maintained isothermally at temperatures of 310 and 285 K, respectively. Velocity profiles are plotted at the mid-section of the cavity as shown in Fig. 3.

From Fig. 3, it is very clear that grid size 61×61 and 81×81 gave same results for velocity magnitude. It is further validated with experimental results [14] for pure water and three different hot wall temperatures (310, 329

and 345 K), respectively. The results are compared in terms of Nusselt number and Rayleigh number which are in agreement with the experimental findings. The temperature distribution profile along the x-axis of the cavity is nearly constant due to the presence of thermal stratification in vertical direction caused by the convective flow near the hot and cold wall respectively.

5.2 For pure water ($\phi = 0$) case

Numerical simulations were carried out for pure water. Fig. 4 shows the numerical result validated against experimental values for 0% volume fraction. Nusselt number was calculated for three different Rayleigh number corresponding to three different temperatures of 310, 329 and 345 K at hot wall and constant temperature of 285 K at cold wall.

The computed results are seen to be in good agreement with the experimental results. As expected, both the computational and experimental results show increase in Nusselt number with increase in Rayleigh number. Figure 5 shows the temperature profiles for pure water at mid-section of the square cavity at three different wall temperatures for pure water.

From Figs. 4 and 5, it is observed that both experimental and numerical simulation for grid size 61×61 are in good agreement. Thus, grid size of 61×61 was used in all other simulations. It should be noted that the Rayleigh's number used in computations are different from experimental values due to difference in the values of material properties (density, viscosity, thermal conductivity and thermal expansion coefficient).
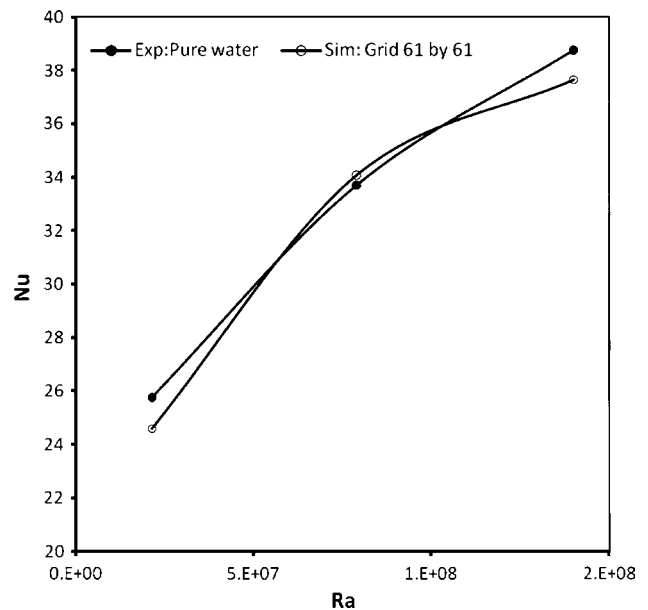

Fig. 3 Grid independent study showing velocity magnitude at mid square cavity

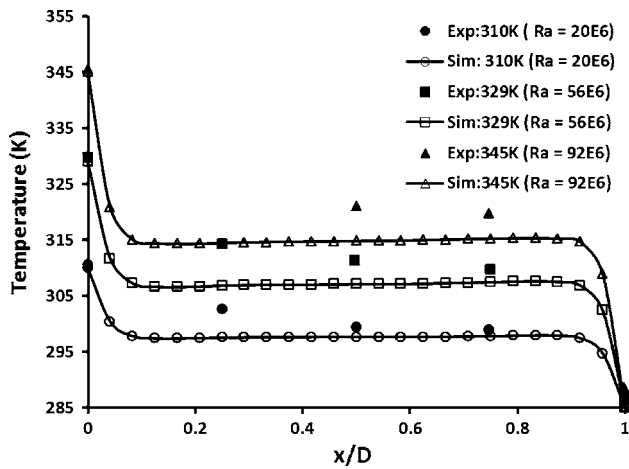**Fig. 4** Nusselt number versus Rayleigh number for pure water

Fig. 5 Temperature profiles at different hot wall temperatures for pure water (grid size 61 by 61)

5.3 For 1% volume fraction

It is seen from Fig. 6 that when the nanoparticles are added to pure water, the Nusselt number decreases compared to that of pure water. The numerical results predict the similar trend as that of the experimental results. However, some discrepancy was observed between experimental and numerical results. Both the models (Kinetic and Maxwell–Garnett) predict the similar trend as observed from the experimental results. Also, both the model gives similar results for Nusselt number as there is little difference in the value of thermal conductivity predicted by both the models. The accuracy depends upon the theoretical model employed for thermal conductivity of nanofluids.
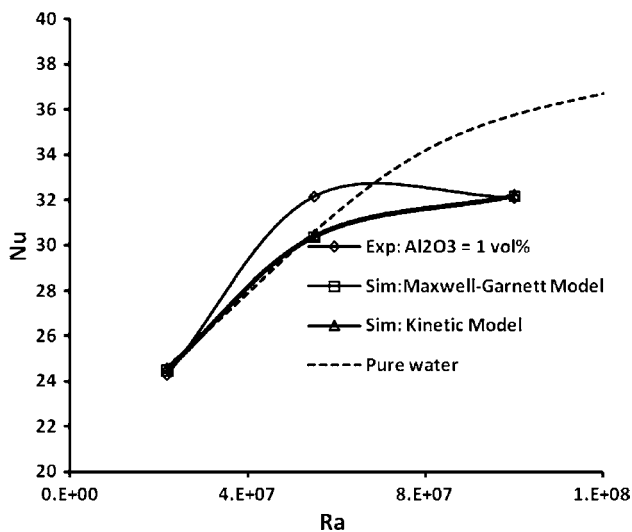
5.4 For 4% volume fraction

Figure 7 represents variation of Nusselt number with Rayleigh number for 4% volume fraction of nanoparticle.

When the volume fraction of the nanoparticles is increased from 1 to 4%, the numerical solutions still exhibits the same trend as observed in the experimental results. Nusselt number decreases with increase in volume fraction of nanoparticles. It can also be observed from comparing with Fig. 6. This phenomenon is paradoxical which is pointed out by [12]. Conventionally, thermal conductivity should increase with increase in volume fraction of the particles, thus, increasing the heat transfer. However, both the experimental and numerical results show degradation in heat transfer in natural convection. One of the reasons explained by [14] is due to slip between the nanoparticles and the fluid particles which disturb the suspension of the nanoparticles inside the liquid, especially at very low velocity natural convection flow. However, comparison of Figs. 6 and 7 shows that, increase in particle volume fraction to 4%, a considerable difference in experimental and numerical results are observed. This may be due to the selection of single phase approach which takes into account the effective mixture properties but not the particles into consideration.

It is further observed that Maxwell–Garnett model shows slightly higher value of Nusselt's number due to the higher thermal conductivity value predicted by the model compared to Kinetic model. The experimental results shows decrease in heat transfer when the concentration of nanoparticles is increased to 4 vol%. However, there is negligible difference in computational results between
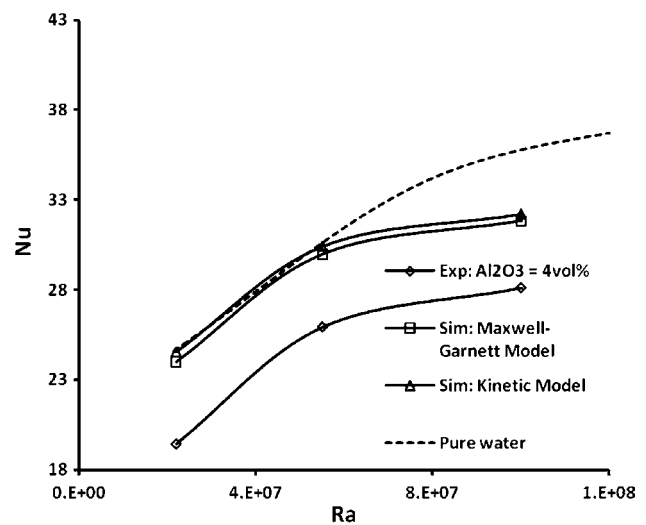

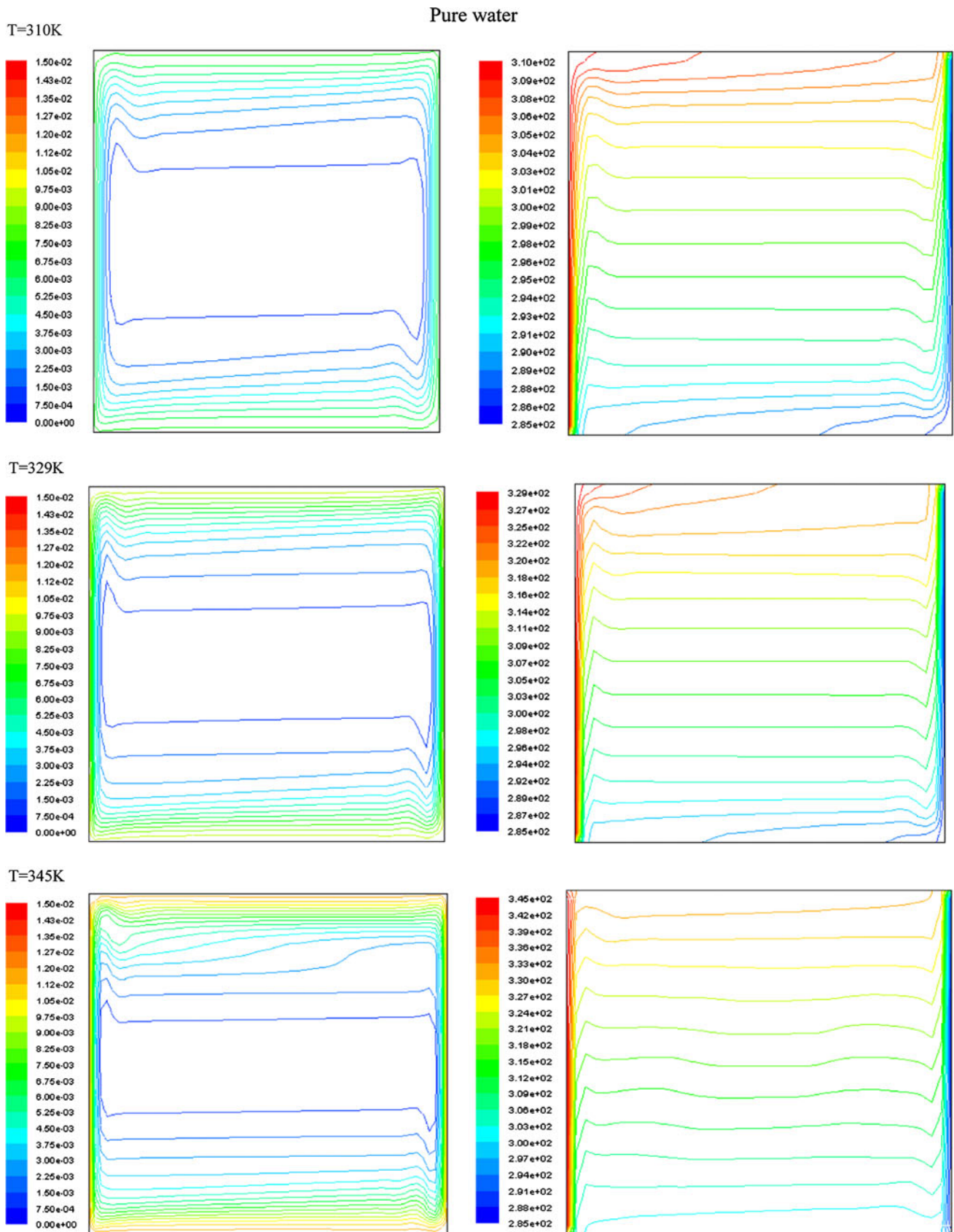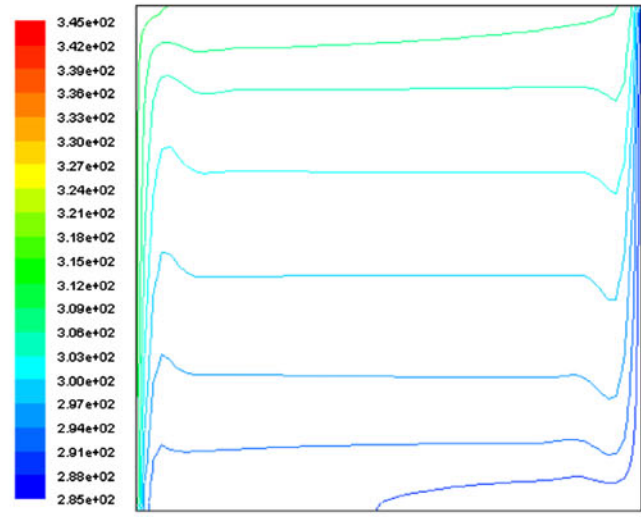**Fig. 6** Nusselt number versus Rayleigh number for 1% volume fraction of Al_2O_3

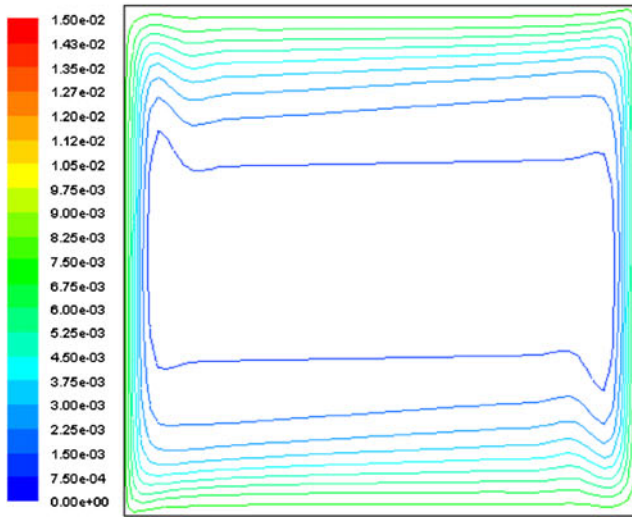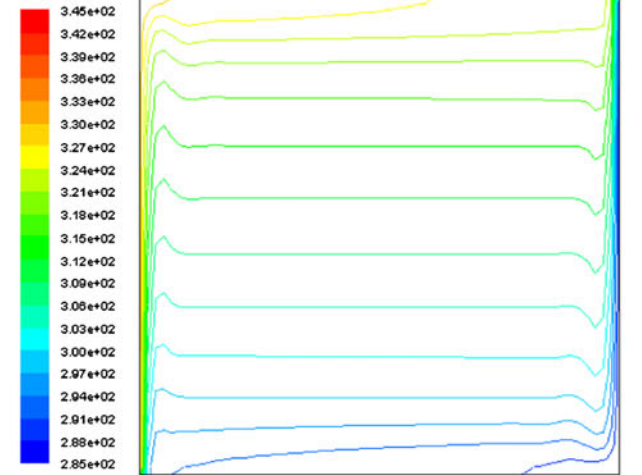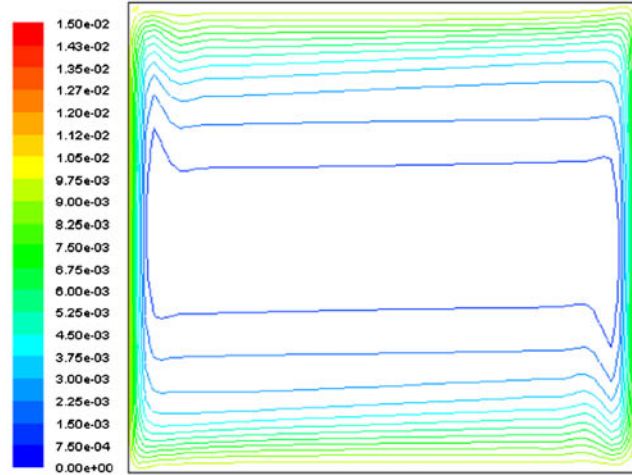**Fig. 7** Nusselt number versus Rayleigh number for 4% volume fraction of Al_2O_3

Fig. 8 Streamline and isotherm for pure water, Al_2O_3 volume fraction of 1 and 4%

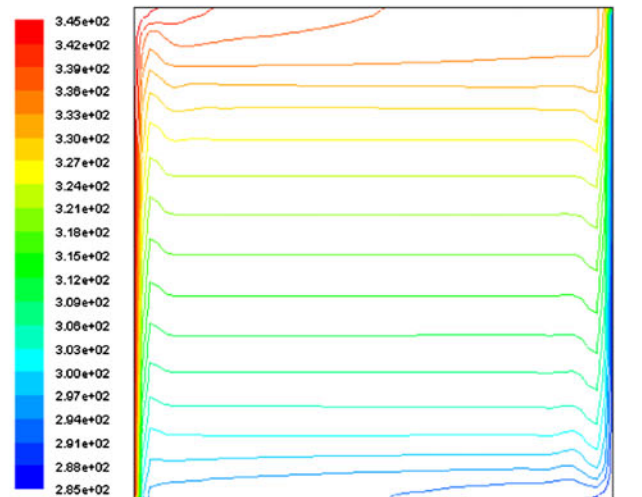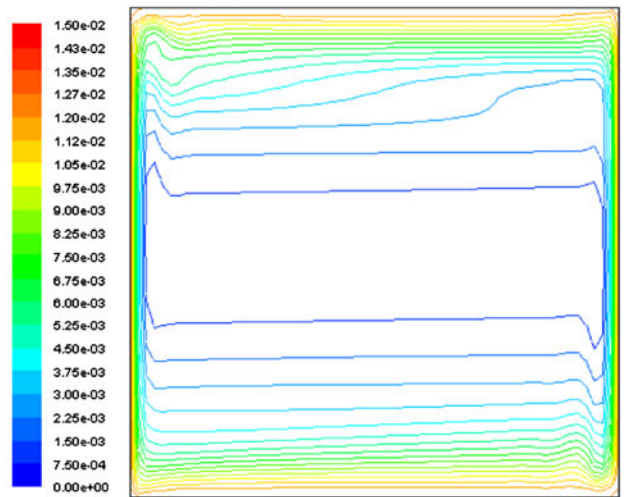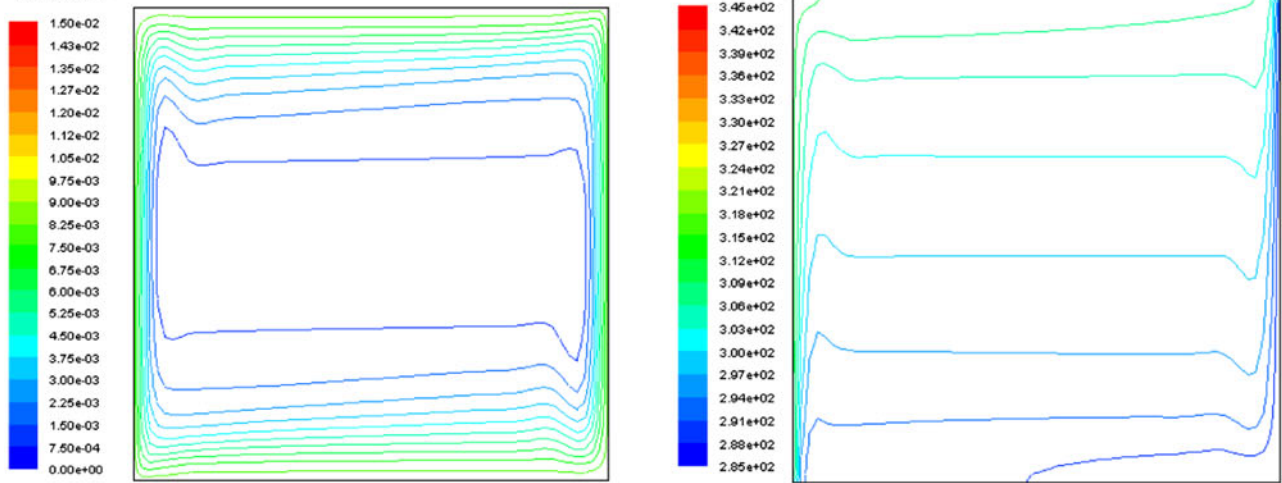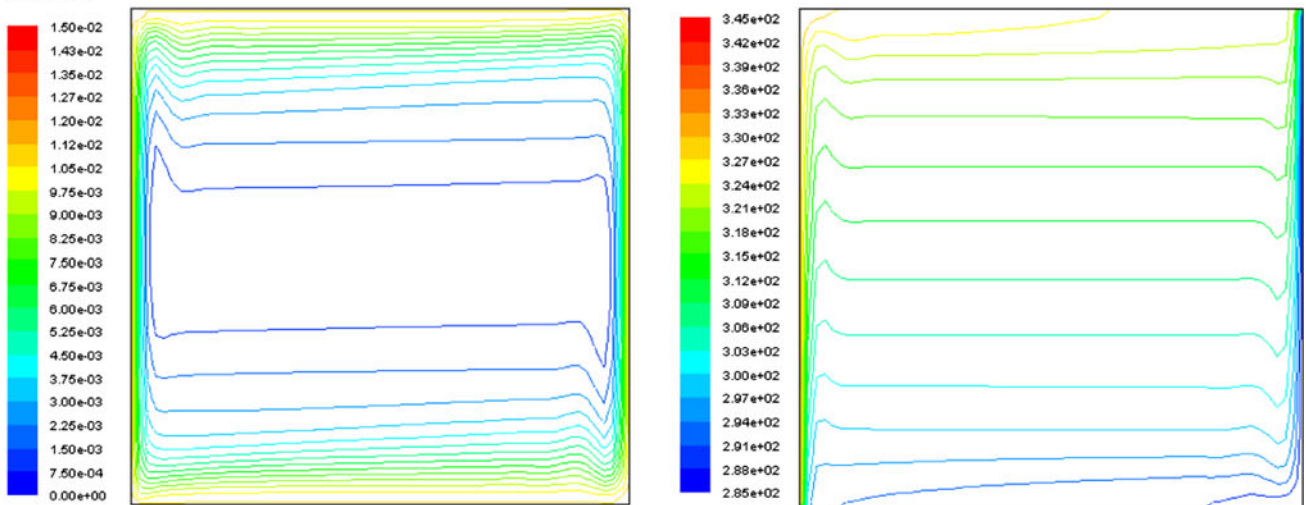At Al$_2$O$_3$ volume fraction = 1%

At 310K

At 329K

At 345K

Fig. 8 continued

At Al$_2$O$_3$ volume fraction = 4%
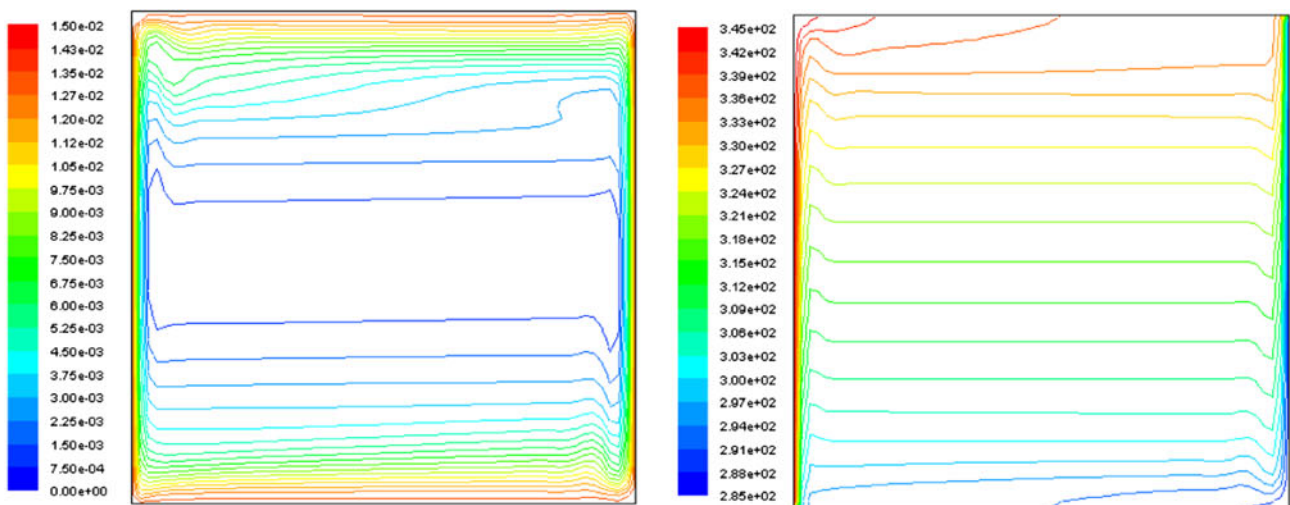
At 310K

At 329K

At 345K

Fig. 8 continued

1 and 4 vol% of nanoparticles which clearly demonstrates that effect of particles, Brownian motion of particles have to be considered in order for us to accurately predict the heat transfer mechanism in natural convection utilizing nanofluids. Another, reason may be due to the adoption of single phase approach assuming that both the fluid and particles are uniformly suspended. However in reality there could be some sedimentation and agglomeration of nanoparticles which can cause difference in computed results especially at higher particle concentrations. Thermal conductivity models used in numerical work also plays a vital role in determining the accuracy of computed results. It is well documented in literature that thermal conductivity of nanofluids is a function of temperature and thus models used in this present work to calculate effective thermal conductivity does not take this into account.

5.5 Streamlines and isotherms

Figure 8 represents streamlines and isotherms for pure water, nanoparticle concentration of 1 and 4%, respectively. It is observed that with increase in hot wall temperature (Ra number), flow rate at the center of circulation increases while the temperature drops very gradually from top to bottom. Further, an energy exchange rate increases due to random and irregular movement of fluid molecules which enhances the thermal dispersion. Furthermore, the flow rates at the center of the enclosure are very small compared to the close to boundaries where fluid is moving at higher velocities.

6 Conclusion

Natural convection heat transfer of nanofluid was studied for Al_2O_3-water in a horizontal cylinder of $L/D = 1.0$ using CFD approach. Single phase model was successfully employed to analyze heat transfer performance of nanofluids using effective properties. Numerical simulations were compared with the experimental results at various values of Rayleigh number which show similar trend and are in reasonable agreement. Both the models show similar results for Nusselt number. Thus, CFD can be effectively implemented for simulations of nanofluid with further improvement over theoretical models that can account for temperature effects. More accurate results can be obtained by taking into account the presence of nanoparticles in consideration.

References

1. Lee S, Choi SUS, Li S, Eastman JA (1999) Measuring thermal conductivity of fluids containing oxide nanoparticles. ASME J Heat Transf 121:280–289
2. Xuan Y, Li Q (2000) Heat transfer enhancement of nanofluids. Int J Heat Fluid Flow 21:58–64
3. Eastman JA, Choi SUS, Li S, Thompson LJ, Lee S (1997) Enhanced thermal conductivity through the development of nanofluids. In: Komarneni S, Parker JC, Wollenberger HJ (eds) Nanophase and nanocomposite materials II. MRS, Pittsburg, pp 3–11
4. Eastman JA, Choi SUS, Li S, Yu W, Thompson LJ (2001) Anomalously increased effective thermal conductivities of ethylene glycol-based nano-fluids containing copper nano-particles. Appl Phys Lett 78:718–720
5. Choi SUS, Zhang ZG, Yu W, Lockwood FE, Grulke EA (2001) Anomalous thermal conductivity enhancement in nano-tube suspensions. Appl Phys Lett 79:2252–2254
6. Das SK, Putra N, Thiesen P, Roetzel W (2003) Temperature dependence of thermal conductivity enhancement for nanofluids. ASME J Heat Transf 125:567–574
7. Khanafer K, Vafai K, Lightstone M (2003) Buoyancy driven heat transfer enhancement in a two-dimensional enclosure utilizing nanofluids. Int. J Heat Mass Transf 46:3639–3653
8. Jang SP, Choi SUS (2004) Free convection in a rectangular cavity (Benard convection) with nanofluids. In: Proceedings of the IMECE, Anaheim, California, USA
9. Jou RY, Tzeng SC (2006) Numerical research of natural convective heat transfer enhancement filled with nanofluids in rectangular enclosures. Int Commun Heat Mass Transf 33:727–736
10. Santra AK, Sen S, Chakraborty N (2008) Study of heat transfer augmentation in a differentially heated square cavity using copper–water nanofluid. Int J Thermal Sci 47:1113–1122
11. Hwang KS, Lee JH, Jang SP (2007) Buoyancy-driven heat transfer of water-based Al_2O_3 nanofluids in a rectangular cavity. Int J Heat Mass Transf 50:4003–4010
12. Jafari A, Mousavi SM, Tynjala T, Sarkomaa P (2009) CFD simulation of gravitational sedimentation and clustering effects on heat transfer of a nano-ferrofluid. In: PIERS proceedings, Beijing, China, March 23–27
13. Ismail AF, Rashmi W, Khalid M (2008) Numerical study on buoyancy driven heat transfer utilizing nanofluids in a rectangular enclosure. In: Proceedings of the UK-Malaysia engineering conference 2008, London, 118–123
14. Putra N, Roetzal W, Das SK (2003) Natural convection of nanofluids. J Heat Mass Transf 39(8–9):775–784
15. Maxwell-Garnett JC (1904) Colours in metal glasses and in metallic films. Philos Trans Roy Soc A 203:385–420
16. Eastman JA, Phillpot SR, Choi US, Keblinski P (2000) Thermal transport in nanofluids. Annu Rev Mater Res 34:219–246